

Two-Dimensional Spatio-Temporal Signal Processing for Dispersion Compensation in Time-Stretched ADC

Alireza Tarighat, *Member, IEEE*, Shalabh Gupta, *Student Member, IEEE*, Ali H. Sayed, *Fellow, IEEE*, and Bahram Jalali, *Fellow, IEEE*

Abstract—Time-stretched analog-to-digital converters (ADCs) have offered revolutionary enhancements in the performance of electronic converters by reducing the signal bandwidth prior to digitization. An inherent limitation of the time-stretched ADC is the frequency-selective response of the optical system that reduces the effective number of bits for ultrawideband signals. This paper proposes a solution based on spatio-temporal digital processing. The digital algorithm exploits the optical phase diversity to create a flat RF frequency response, even when the system's transfer function included deep nulls within the signal spectrum. For a $10\times$ time-stretch factor with a 10-GHz input signal, simulations show that the proposed solution increases the overall achievable signal-to-noise-and-distortion ratio to 52 dB in the presence of linear distortions. The proposed filter can be used to mitigate the dispersion penalty in other fiber optic applications as well.

Index Terms—Analog-to-digital conversion (ADC), optical signal processing, spatio-temporal digital processing, time-stretched converters.

I. INTRODUCTION

DIGITIZING ultrawideband analog signals in real time is a challenging task in many applications such as communications, radar systems, and precise measurements. A sampling oscilloscope (as opposed to a real-time digitizing oscilloscope) is not an option since it requires the signal to be repetitive in time. It only provides information about the average signal behavior; hence, it does not operate in real time. Real-time capture of ultrafast electrical signals is a difficult problem that requires wideband analog-to-digital converters (ADCs) [1]. The standard approach to design ultrafast converters is to employ parallelism through the use of a time-interleaved ADC architecture [2], [3]. This architecture can also be implemented using an optical sampling where a mode-locked laser combined with an electrooptic modulator provides low jitter and fast sampling of the electrical waveform [4], [5]. The signal is captured by

Manuscript received March 18, 2006; revised January 24, 2007. This work was supported by Defense Advanced Research Projects Agency (DARPA). Part of this paper was presented in the *Proceedings of the IEEE MTT-S International Microwave Symposium (IMS)*, 2007.

A. Tarighat was with the Electrical Engineering Department, University of California, Los Angeles, CA 90095 USA. He is now with WiLinX, Los Angeles, CA 90025 USA (e-mail: tarighat@ee.ucla.edu).

S. Gupta, A. H. Sayed, and B. Jalali are with the Electrical Engineering Department, University of California, Los Angeles, CA 90095 USA (e-mail: shalabh@ee.ucla.edu; sayed@ee.ucla.edu; jalali@ee.ucla.edu).

Color versions of one or more of the figures in this paper are available online at <http://ieeexplore.ieee.org>.

Digital Object Identifier 10.1109/JLT.2007.896758

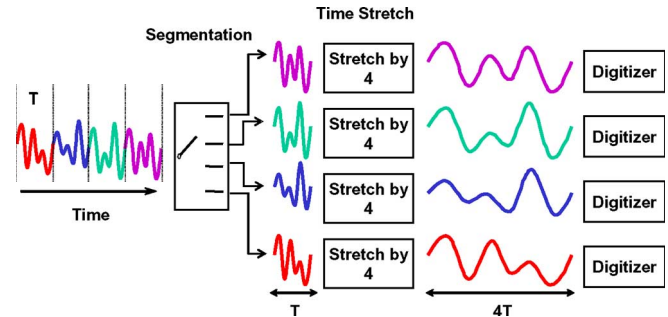


Fig. 1. TS-ADC concept.

a parallel array of slow digitizers, each clocked at a fraction of the Nyquist rate. A state-of-the-art electronic ADC, which is embodied by real-time digitizing oscilloscopes (Tektronix TDS7404 or Agilent 54854A), boasts 20-GSamples/s 6-GHz analog bandwidth. Depending on the input-signal amplitude, these instruments only exhibit an effective number of bits (ENOB) of approximately 4 to 5.5 b.

An entirely different ultrafast ADC architecture is the so-called time-stretched ADC (TS-ADC) shown in Fig. 1 [6]–[8], [10]. The analog signal is slowed down prior to sampling and quantization by an electronic digitizer. A practical method for implementing the time-stretch function is to use the photonic technique [8]–[10]. A linearly chirped optical pulse is generated by propagating the broadband pulses generated by a supercontinuum source in a chromatic dispersive medium such as the single mode fiber [11]. The electrical input signal modulates the intensity of the chirped optical pulses in an electrooptic modulator (see Fig. 2). The envelope is subsequently stretched in a second spool of fiber before photodetection and digitization by a moderate-speed electronic ADC.

While fiber dispersion performs the desired function of time stretch, it has also adverse influences on the electrical signals. More specifically, the influence of the linear dispersion on the spectral shape spectrum of the electrical signal has been analyzed in [10]. It was shown that the linear dispersion will result in a frequency-selective response in the time-stretched electrical signal as the equivalent electrical domain frequency response is shown in Fig. 3. The frequency-selective nature of the system response limits the integrity of the electrical signal and, consequently, the achievable resolution, as quantified by ENOB. As will be shown in the simulation section, the ENOB achievable by the system in [10] is limited to 5 b at

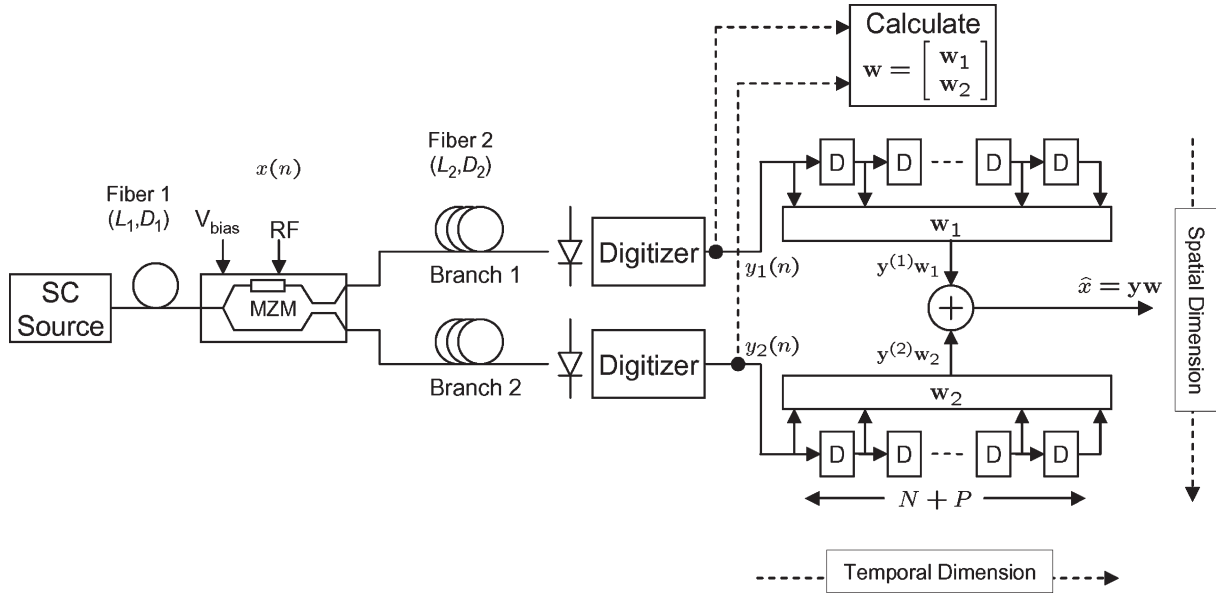


Fig. 2. Block diagram of the TS-ADC with dual branches and the proposed 2-D spatio-temporal digital processing.

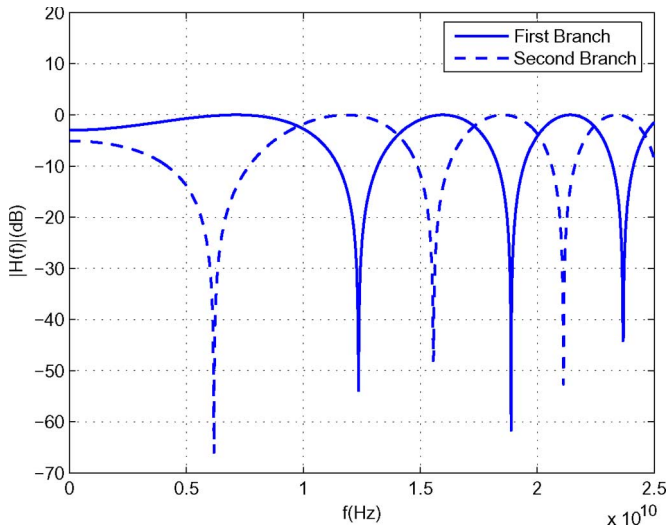


Fig. 3. Frequency transfer functions of the optical branches.

1-GHz signal bandwidth, and it sharply drops as the bandwidth increases beyond 1 GHz.

In this paper, we propose a digital spatio-temporal¹ filter that eliminates the RF bandwidth limitation. Applied to a two-port Mach-Zehnder modulator, it exploits the optical phase diversity to create a flat RF frequency response. As will be shown in the simulation section, the signal-to-noise-and-distortion ratio (SNDR)² is improved to more than 52 dB at up to 10-GHz signal bandwidth. This improvement in performance comes at the cost of the additional postdigitizer signal processing. Considering the rapid scale down in very-large-scale-integration (VLSI) technology, the additional cost due to the digital processing is

¹The term “spatial” refers to the fact that there are two spatially separate Mach-Zehnder channels that are being processed. It is also the terminology used in the signal processing literature when multichannel systems are described.

²More precisely, the term SNDR refers to signal-to-quantization-noise-and-distortion-ratio (SQNDR) throughout this paper.

well justified and minimal compared to the cost of the optical components. Although the proposed 2-D signal processing is only applied to the TS-ADC in this paper, however, it can be potentially applied to other optical systems that require a highly flat frequency response. While the proposed 2-D algorithm is aimed at compensating the frequency-selective linear distortion in the system, nonlinear harmonic distortions can be another limiting factor. To study this issue, the effect of harmonic distortions on the SNDR is discussed in details and quantified for the system configuration under study. Furthermore, it is shown that the degradation due to harmonic distortions can be managed by using a suboctave regime.

This paper is organized as follows. The next section provides an overview of the optical TS-ADC. Section III describes the proposed 2-D signal-processing scheme. Simulation results are shown in Section IV. The harmonic distortions are discussed in Section V, and the conclusion is given in Section VI.

II. OPTICAL TS-ADC

In this section, we provide a brief overview of the optical TS-ADC concept derived from [10]. The stretch process consists of two steps. Step one is the time-to-wavelength (t -to- λ) mapping performed by the combination of the chirped optical pulse and the electrooptic modulator. Nearly transform-limited optical pulse, which is generated by a supercontinuum source, is chirped after propagating through a dispersive medium. When this chirped pulse is modulated by an intensity modulator, the time-domain signal is mapped into wavelength domain. Step two is the wavelength-to-time (λ -to- t) mapping performed by the second fiber. The modulated chirped pulse propagates through a second dispersive medium. As a result, the signal modulated onto the chirp pulse is stretched in the time.

While dispersion performs the desired function of time stretch, it has other influences on the electrical signals. The linear dispersion results in a frequency-dependent attenuation as well as frequency-dependent harmonic distortion in the

time-stretched electrical signal [10]. Let L_1 and L_2 denote the lengths of the first and second fibers, respectively. The magnification or time-stretch factor is then given as $M = 1 + L_2/L_1$. It is shown generally that $M = 1 + D_2/D_1$, where D_1 and D_2 are the total dispersion in the first and second dispersive elements, respectively. However, the stretched signal passes through a frequency-dependent channel described by [10]

$$H_1(f) = \cos^2 \left(\phi_{\text{DIP}} - \frac{\pi}{4} \right) \quad (1)$$

where ϕ_{DIP} is the dispersion induced phase (DIP) defined as

$$\phi_{\text{DIP}} = 2\pi^2 \beta_2 \frac{L_2}{M} f^2. \quad (2)$$

The aforementioned transfer function is plotted in Fig. 3 for $\beta_2 = -21.67 \text{ ps}^2/\text{km}$, $L_1 = 5 \text{ km}$, $L_2 = 45 \text{ km}$, and $M = 1 + L_2/L_1 = 10$. The deep fades in this transfer function severely degrade the integrity of the electrical signal being sampled. Although this transfer function looks relatively flat at least at low frequencies, however, there will be a large ENOB penalty, even at low frequencies (as will be shown in the next section). This occurs because if we are interested in a wide dynamic range, a slight frequency rolloff in the signal bandwidth (and, consequently, a slight signal distortion) results in a large penalty in dynamic range.

To address this problem, a dual-branch system was proposed by Han *et al.* [12]. By using a single-arm Mach–Zehnder modulator which gives opposite polarity chirped modulation to the two branches, the stretched electrical signal experiences a different attenuation through the second branch, which is given by

$$H_2(f) = \cos^2 \left(\phi_{\text{DIP}} + \frac{\pi}{4} \right). \quad (3)$$

The aforementioned transfer function is plotted in Fig. 3 for the same parameters. Fortunately, as shown from the figure, the frequency fading in the two ports is complementary. As pointed out by Han *et al.*, this occurs due to the optical phase diversity in the two outputs and can potentially be used to eliminate the dispersion penalty. The problem that was not addressed is how to combine and process the two ports to achieve the maximum performance. Potentially, the complementary nature of the two transfer functions can be exploited to recover the original wideband electrical signal despite the deep fades in individual branches.

Different approaches can be considered to address the problem.

- 1) One simple approach would be to select the branch with the flatter response at lower frequencies, i.e., the branch shown in Fig. 3. However, the slight frequency rolloff in the signal bandwidth results in a large unacceptable penalty in SNDR as is shown in the simulation section.
- 2) As an incremental improvement, an equalization technique can be applied on a single branch to recover the original desired data. However, using an equalization technique will still result in a degradation in SNDR, as shown in the simulation section. At high target per-

formance and even in the presence of equalization, the SNDR will still be limited by the frequency-selective response of the channel rather than the dynamic range of the quantizers used in the system.

- 3) One other approach would be to channelize the band of interest into smaller subbands such that the frequency response of the branches can be considered flat within each subband. In this case, the wideband signal of interest needs to be decomposed into many narrowband signals. Then, each narrowband signal corresponding to a different frequency point is combined with different coefficients, depending on the channel responses at each frequency point. More precisely, once the signal is transformed into subbands in the frequency domain, a maximal-ratio-combining technique in the frequency domain can be used where the combining coefficients will then be frequency dependent.

There are major drawbacks with the channelization approach. Due to high sensitivity of ENOB to frequency rolloffs, the subbands will need to become extremely narrow which will indeed require a very large number of subbands on the order of thousands (which will become impractical for ultrawideband signals). Additionally, channelizing an ultrawideband signal into a large number of subbands will require a large amount of processing, even if the fast Fourier transform (FFT) and the inverse FFT are used for channelization.

On the other hand, any approach that relies on the exact transfer functions (1) and (3) will suffer from severe degradation due to any possible slight mismatch between (1) and (3) that, in practice, arises due to imperfections in the Mach–Zehnder modulator. A practical approach should be robust to any deviation/mismatch from these theoretical models in practice and should be able to adapt to such variations and mismatches. Up to now, a suitable and efficient solution did not exist, and although the potential of the diversity has been discussed [12], it could not be exploited. In other words, the full potential of the TS-ADC system will not be fully utilized until the frequency-selective distortion inherent in the system is eliminated.

III. COMPENSATION ALGORITHM

In this paper, we propose a 2-D spatio-temporal digital processing technique to eliminate the dispersion penalty in the optical TS-ADC. The available diversity in different paths is exploited through a 2-D receiver structure. The proposed scheme has the following key features.

- 1) It implements the globally optimum linear estimator in the minimum mean-square-error (MMSE) sense. The proposed scheme leads to a jointly optimized solution in both space and time.
- 2) It provides a computationally efficient solution compared to the channelization approach.
- 3) Using a training phase, it adaptively adjusts to the frequency characteristics of the two branches of the modulator and, therefore, is robust to any deviations/mismatches between the branches.

Let $x(n)$ represent the original data being sampled by the TS-ADC. Furthermore, let $y_1(n)$ and $y_2(n)$ be the received data on the two branches, respectively. Assuming that an equalizer of forward length N and backward length P is used (a total length $N + P$), then

$$\mathbf{y}^{(1)} = \begin{bmatrix} y_1(n+P) \\ y_1(n+P-1) \\ \vdots \\ y_1(n) \\ \vdots \\ y_1(n-N) \end{bmatrix}^T, \quad \mathbf{y}^{(2)} = \begin{bmatrix} y_2(n+P) \\ y_2(n+P-1) \\ \vdots \\ y_2(n) \\ \vdots \\ y_2(n-N) \end{bmatrix}^T. \quad (4)$$

Now, the problem becomes recovering $x(n)$ from data vectors $\mathbf{y}^{(1)}$ and $\mathbf{y}^{(2)}$. To derive a globally optimum linear estimator, we form the following row vector:

$$\mathbf{y} = [\mathbf{y}^{(1)} \quad \mathbf{y}^{(2)}] \quad (5)$$

and the estimation problem becomes

$$\hat{x}(n) = \mathbf{y}\mathbf{w} \quad (6)$$

where $\hat{x}(n)$ is the recovered $x(n)$, and the column vector \mathbf{w} is the combining coefficients of size $2(N + P)$. We will use the term ‘‘temporal’’ to refer to the processing performed on the individual $\mathbf{y}^{(1)}$ and $\mathbf{y}^{(2)}$ vectors along the time dimension. We will use the term ‘‘spatial’’ to refer to the processing performed on the corresponding entries of $\mathbf{y}^{(1)}$ and $\mathbf{y}^{(2)}$ vectors, i.e., $(y_1(k), y_2(k))$, along the space dimension. Therefore, the term ‘‘spatio-temporal’’ refers to the solution that performs the digital processing on both dimensions jointly.

Different techniques (adaptive and otherwise) can be used to calculate \mathbf{w} . The solution corresponding to the MMSE linear estimator is given by [13]

$$\mathbf{w} = R_{\mathbf{y}}^{-1}R_{x\mathbf{y}} \quad (7)$$

where

$$R_{x\mathbf{y}} = \mathbf{E}x\mathbf{y}^* \\ R_{\mathbf{y}} = \mathbf{E}\mathbf{y}\mathbf{y}^*$$

are the cross correlation and covariance matrices, respectively. In practice, time averaging over multiple blocks of x and \mathbf{y} can be used to estimate these matrices. Let us introduce the time (or iteration) index i such that x_i and \mathbf{y}_i^* represent the values of x and \mathbf{y}^* at time instant i . Then

$$R_{x\mathbf{y}} \approx \frac{1}{T} \sum_{i=1}^T x_i\mathbf{y}_i^* \\ R_{\mathbf{y}} \approx \frac{1}{T} \sum_{i=1}^T \mathbf{y}_i^*\mathbf{y}_i \quad (8)$$

where T is the number of training blocks available.

For more hardware-friendly implementations, adaptive algorithms can be used to calculate \mathbf{w} recursively. For instance, the

recursive-least-square (RLS) algorithm can be used [13]

$$\begin{cases} \mathbf{w}_i = \mathbf{w}_{i-1} + \mathbf{P}_i\mathbf{y}_i^* [x(i) - \mathbf{y}_i\mathbf{w}_{i-1}] \\ \mathbf{P}_i = \lambda^{-1} \left[\mathbf{P}_{i-1} - \frac{\lambda^{-1}\mathbf{P}_{i-1}\mathbf{y}_i^*\mathbf{y}_i\mathbf{P}_{i-1}}{1 + \lambda^{-1}\mathbf{y}_i\mathbf{P}_{i-1}\mathbf{y}_i^*} \right] \end{cases} \quad (9)$$

for $i \geq 0$ with initial conditions $\mathbf{w}_0 = \mathbf{0}$, $\mathbf{P}_{-1} = \epsilon^{-1}\mathbf{I}$, and $0 \ll \lambda \leq 1$. The scalar ϵ is usually a small positive number, and λ is usually close to one. Furthermore, $x(i)$ is a known sequence during the training phase.

Note that the term ‘‘adaptive’’ also refers to the ‘‘recursive’’ nature of the proposed adaptive algorithm. In other words, the adaptive algorithm is a computationally efficient and a numerically stable way of implementing the original optimal MMSE solution. This is in addition to the fact that the algorithm has the capability to adapt to the variations in the channel if they happen at a slower rate than the algorithm’s convergence rate. The adaptive method starts from an all-zero coefficient initial state without a need of any knowledge about the real transfer function of the system. This is a key advantage of the adaptive (or recursive, in that sense) algorithms where they use a training period to adaptively converge to the MMSE solution. Note that neither MMSE nor adaptive solution relies on the exact transfer functions of the system. They both use some training phase to learn about the response of the system and compensate for its effect. Any solution that directly relies on the theoretical response of the system is highly impractical and unfeasible. The difference between the two solutions is as follows: 1) the computationally efficient nature of the adaptive solution; 2) the numerical stability of the adaptive algorithm in real-world hardware implementations; and 3) the adapting nature of the adaptive algorithm to environmental changes during the updates.

Following describes briefly how the performance of the system in terms of ENOB is quantified. Once the bandlimited signal $x(n)$ is passed through the optical time-stretching system, it is sampled by the electronic quantizer. The quantizer adds a quantization noise to the received signal with a signal-to-quantization-noise-ratio (SQNR) equal to $6.02N_Q + 1.76$ in decibels, where N_Q is the number of the quantizer’s bits [14]. The proposed signal-processing scheme is then applied to the quantized received signals in order to recover the original desired signal $x(n)$, where the recovered sequence is denoted by $\hat{x}(n)$. In addition to the quantization noise, a distortion is also added to the final sampled signal due to the frequency response of the system. We define the signal-to-quantization-noise-and-distortion-ratio (SQNDR) quantity to capture both these effects. The final processed SQNDR is calculated according to

$$\text{SQNDR} = \frac{\mathbf{E}x^2}{\mathbf{E}(\hat{x} - x)^2} \quad (10)$$

and the ENOB is calculated as

$$\text{ENOB} = \frac{\text{SQNDR} - 1.76}{6.02} \quad (11)$$

where the SQNDR is stated in decibels. Note that the SQNDR values used in calculating the ENOB figures in this paper only

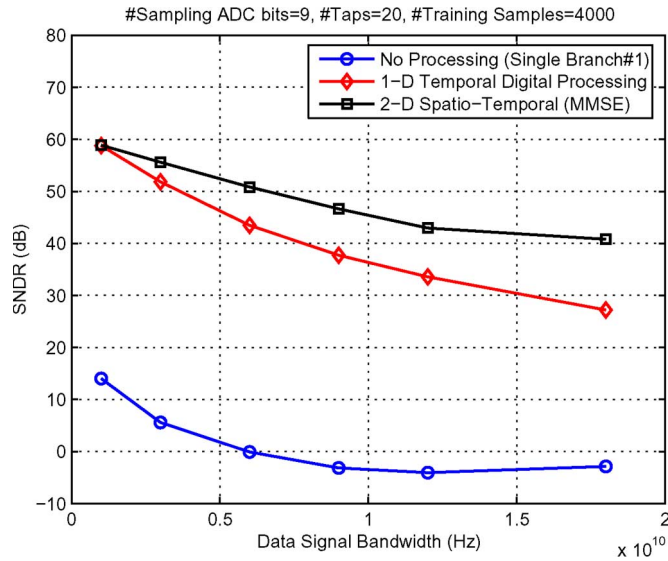


Fig. 4. SNDR versus the signal bandwidth. The following parameters are used: Number of training samples = 4000, number of sampling quantizer bits $N_Q = 9$, and number of taps $N + P = 20$. The equivalent ENOB can be calculated according to (11).

take into account the frequency-selective distortion, and the nonlinear effects are not reflected in the results.

The degradation in SQNDR versus signal bandwidth is mainly due to the frequency-selective distortion rather than the quantization noise. Therefore, although the SQNDR (and, consequently, the ENOB) at the output of each individual branch is poor (see Figs. 4 and 5), the SQNR at each individual branch is sufficiently high for the postprocessing algorithm to function. In other words, while each branch quantizer individually is not capable of providing a version of the original signal with acceptable ENOB resolution, it can, however, provide a high-resolution version of the distorted signal of interest such that the 2-D processing can reconstruct the original signal with high equivalent ENOB. While the SQNR at the output of each branch is with high quality, the SQNDR at the output of each branch drops rapidly to below 1 dB due to the highly frequency-selective response of the optical system. The signal processing algorithm is able to reconstruct the distorted signal from the branch outputs (with a low SQNDR) since they come with high SQNR (where the SQNR is only limited by the electronic quantizer number of bits).

Consider the frequency components that experience a deep fade through one of the branches. Since the channel gain on such frequencies is low, it would not utilize the full dynamic range of the electronic quantizer and will no longer provide an SQNR equivalent to the full quantization bits. In other words, the digital signal processing algorithm will no longer be able to extract the original signal with the full-quantization-bit quality from that branch alone as that particular frequency. This is in fact the reason that the single-branch 1-D equalization cannot provide a flat performance over all frequencies. The keynote here is the fact that the two different branches are complementary in terms of gain versus frequency (see Fig. 3). The signal frequency components that experience a deep frequency fade through the first branch experience a flat high gain

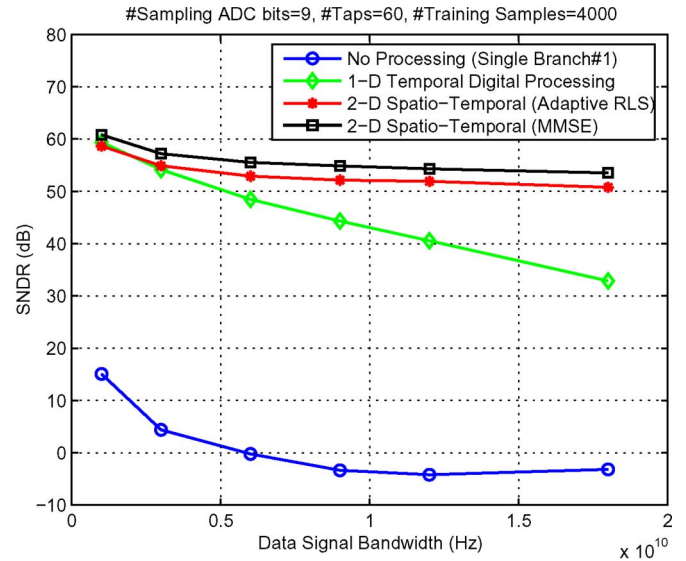


Fig. 5. SNDR versus the signal bandwidth comparing the optimal MMSE solution (7) with the adaptive RLS implementation (9). The following parameters are used: Number of training samples = 4000, number of sampling quantizer bits $N_Q = 9$, and number of taps $N + P = 60$. The equivalent ENOB can be calculated according to (11).

through the second branch, and vice versa. It is in fact the task of the proposed 2-D spatio-temporal digital processing to combine these frequency components from the two branches in an intelligent way to construct the original signal of interest. Intuitively speaking, for frequency components that experience a deep fade through one branch, the 2-D digital processing for that particular frequency component relies mostly (due to its adaptive and trainable nature) on the received signal through the other branch (which has a flat high gain for those particular frequency components).

IV. SIMULATIONS

Simulations are used to validate the effectiveness of the proposed signal processing algorithms. The simulation setup is shown in Fig. 2. The frequency responses given by (1) and (3) are used in the simulations to model the optical system response, and the nonlinear effects are not included in the simulations. The target is to characterize the SNDR as a function of the sampled signal bandwidth. The following are the parameters used in the simulation setup: $\beta_2 = -21.67 \text{ ps}^2/\text{km}$, $L_1 = 40 \text{ km}$, $L_2 = 360 \text{ km}$, and $M = 1 + L_2/L_1 = 10$. The corresponding dispersion parameter is then equal to $D = (-2\pi c/\lambda^2)\beta_2 = 17 \text{ ps/km/nm}$. The resulting frequency-domain behavior of the first and second branches is shown in Fig. 3. A random sequence $x(n)$ is generated, and its spectrum is shaped through a raised cosine low-pass filter with a variable bandwidth. This configuration is used to evaluate the performance of the TS-ADC as a function of the sampled signal bandwidths. The simulation results provided here correspond to a scenario with an arbitrary phase mismatch between the two branches (unknown to the algorithm). This is to show that the adaptive algorithm performs well, even if it does not know the real transfer functions of the branches or if there is some mismatch between the branches.

Simulations are conducted for different scenarios with the following legends.³

- 1) “No Processing”: Single sampling branch is used with no postsampling processing.
- 2) “1-D Temporal Processing”: Single sampling branch is used with 1-D processing in the time domain (equivalent to equalization). In this case, in the solution given by (4)–(6), only one branch $\mathbf{y}^{(1)}$ (corresponding to the branch shown in Fig. 3) is used to recover $x(n)$. The linear estimator given by (7) is used with the approximations given by (8).
- 3) “2-D Spatio-Temporal Processing”: Dual sampling branches are used with joint 2-D processing in both the temporal and spatial domains. In this case, in the solution given by (4)–(6), both branches $\mathbf{y}^{(1)}$ and $\mathbf{y}^{(2)}$ are used to recover $x(n)$. The linear estimator given by (7) is used with the approximations given by (8).
- 4) “2-D Adaptive Processing”: In this case, an adaptive implementation of the “2-D Spatio-Temporal Processing” is simulated according to RLS updates (9).

Now, let us consider the simulation results in Figs. 4 and 5. It is shown that the single-branch structure with no digital signal processing cannot achieve an acceptable ENOB for wideband signals due to the distortion caused by the frequency-selective nature of the system. In other words, a postprocessing scheme is a necessary phase for many practical requirements (see Figs. 4 and 5). While the 1-D temporal processing improves the performance of the system significantly compared to the no-processing scenario, it still cannot guarantee a flat performance for up to 10-GHz bandwidth (see Fig. 5).

The 2-D spatio-temporal MMSE digital processing is a promising approach to achieve a flat SNDR for up to 10-GHz bandwidth (see Fig. 5). This shows that while the TS-ADC has great potential, it still requires advanced signal processing techniques in order to utilize its potential. For more hardware-friendly VLSI implementations, adaptive algorithms such as RLS demonstrate a performance that closely follows that of the optimal MMSE solution (see Fig. 5).

The performance of the compensation scheme depends on the number of taps used in the filter. While $N + P = 20$ is not enough to achieve a consistent and flat performance, $N + P = 60$ is enough to result in a flat SNDR versus signal bandwidth (see Figs. 4 and 5). The achievable SNDR degrades slightly (6–9 dB) as the bandwidth increases, even in the presence of the 2-D processing (see Fig. 5). This is mainly due to the limitation of a finite-impulse-response structure in equalizing the deep-

³The system simulation is performed at a high sampling rate (e.g., 36 GHz) in order to fully capture the high-frequency behavior of the system. However, it is numerically difficult to simulate very low-frequency components (e.g., a low-pass filter) at very high sampling rates. Therefore, the simulation results for the relatively low bandwidth RF signals are not numerically reliable. Furthermore, while we are using 9-b quantizers on each branch, we observe an SNDR of 60 dB at low frequencies. This translates to a 4-dB improvement in SNDR compared to theoretical $6.02 * 9 + 1.76 = 56$ dB per individual branch. Assuming an independent quantization noise on two branches justifies a 3-dB gain in the SNDR after the digital processing. Since the remaining 1-dB difference is observed at an SNDR floor of 56 dB, the authors believe it can be due to some very minor effects such as filtering effects, bandlimited RF/filter modeling, and hidden frequency diversity in the branches.

faded channels. Using a 2-D spatio-temporal infinite-impulse-response structure can further improve this degradation.

We observe that the signal-processing algorithm is capable of creating a flat frequency response, even when deep nulls exist within the signal bandwidth. Hence, while the aforementioned results considered a baseband signal spanning near dc to 10 GHz, it should be clear that the proposed technique will be equally effective for passband signals centered at a higher center frequency. This is so, because the complementary nature of the transfer functions belonging to the two signal branches exists at all frequencies, as is evident in Fig. 3.

Although the proposed 2-D signal processing is only applied to the TS-ADC in this paper, it can, in principle, be applied to other dispersive optical systems that suffer from frequency fading. With the availability of two fiber branches, the scheme can transform the frequency-selective response of an optical system into a highly flat response, even in the presence of severe fiber dispersion.

V. DISPERSION-INDUCED NONLINEARITIES

Dispersion of optical signal plays the crucial role of stretching the RF in time domain. However, as discussed earlier, dispersion also adds frequency-dependent attenuation in the signal transfer function, which can be corrected for by signal processing, as shown in this paper. However, another ill effect caused by dispersion is dispersion induced nonlinearity that causes harmonic and intermodulation distortion [10]. In this section, we discuss the limitation imposed on the achievable ENOB and present schemes to minimize the problem. While the proposed 2-D spatio-temporal digital processing algorithm addresses the linear distortions in the system, the schemes discussed in this section aim at minimizing the effect of nonlinear distortions.

The optical spectrum after the Mach–Zehnder modulator consists of the upper and lower modulation sidebands, as well as the even and odd order distortion tones caused by the modulator’s transfer function. At the detector, these frequency components and the optical carrier beat with each other, producing tones at the fundamental RF frequency as well as its even and odd order intermods and harmonics. In the absence of dispersion, even order tones cancel, leading to the well-known RF spectrum for Mach–Zehnder modulator that has the linear plus odd order distortion components. In the presence of dispersion, even order distortion tones no longer vanish and result, for multioctave signals, in a marked reduction in dynamic range [10].

To illustrate this phenomenon, we recall the output photocurrent for a single tone modulation at the RF frequency [10]

$$I_{\text{out}}(t) = I_{\text{Envelope}}(t) \left(1 - m \cos \phi_{\text{DIP}} \cos \frac{\omega_{\text{RF}} t}{M} + \frac{m^2}{8} (1 - \cos 4\phi_{\text{DIP}}) \cos 2 \frac{\omega_{\text{RF}} t}{M} + \frac{m^3}{96} (\cos 9\phi_{\text{DIP}} + 3 \cos 3\phi_{\text{DIP}}) \times \cos 3 \frac{\omega_{\text{RF}} t}{M} + \dots \right) \quad (12)$$

where $I_{\text{Envelope}}(t)$ is the current that would be received in the absence of any modulation. Numerical simulations of harmonic

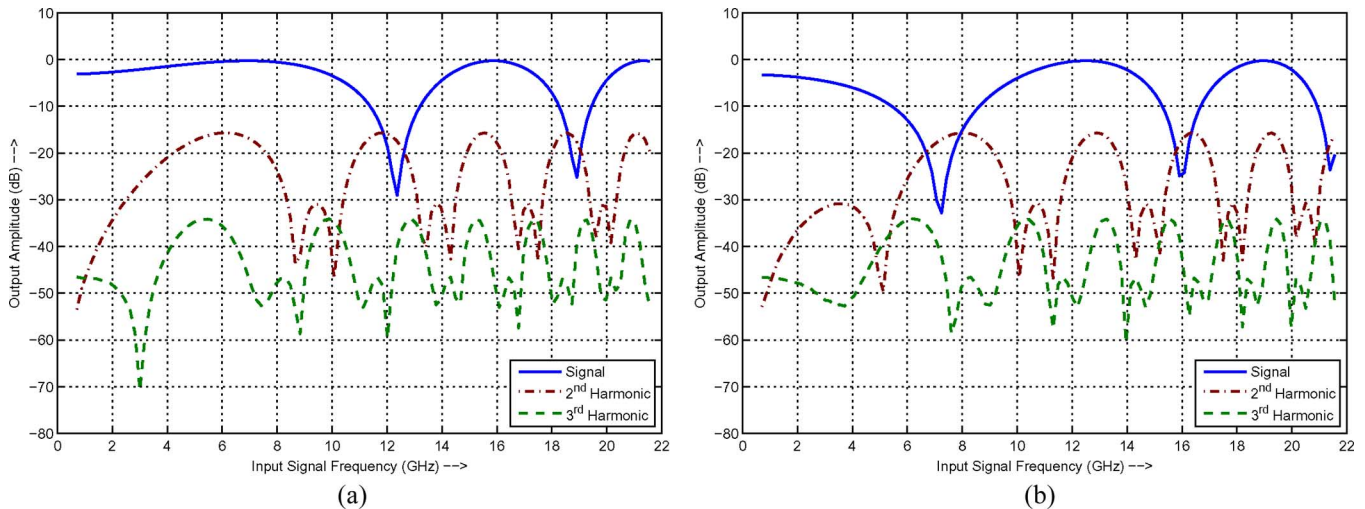


Fig. 6. Frequency transfer functions of the RF signal and its harmonics. (a) First modulator output. (b) Second modulator output.

distortion of RF tone for the two phase diversity outputs are shown in Fig. 6(a) and (b). It is clear from the figures that second-order nonlinearity due to dispersion can severely limit the dynamic range of the system for a wide bandwidth (multi-octave) signal.

As a consequence of this phenomenon, the TS-ADC is best suited for suboctave signals, where the second-order distortion falls outside the signal band. For example, a 10-GHz bandwidth signal spanning the 11–21-GHz band or higher is not corrupted by the second-order intermod and harmonic distortion.

With suboctave bandwidths, the third-order nonlinearities become the limiting factor in the dynamic range of the system. From (12), we find that signal to third harmonic ratio is proportional to m^4 in terms of electrical power. As the third harmonic component is a strong function of modulation depth m , it imposes an upper limit on the modulation depth. The modulation depth cannot be reduced arbitrarily because lowering m degrades the SNR, which is proportional to m^2 [10]. This introduces a tradeoff leading to an optimum value for m . For example, with a modulation depth of 0.2, an SNR of approximately 50 dB can be achieved. Simulations of two-tone intermod distortion shown in Fig. 7 show a similar value for the signal-to-distortion ratio. Achieving higher dynamic range will require linearization of the modulator's transfer function, which is a subject that is beyond the scope of this paper.

Ideally, the Mach–Zehnder modulator is always biased at quadrature point. However, there can be small bias offsets that introduce significant second-order nonlinearity in the link. Mach–Zehnder bias control, which can be achieved using several techniques including one discussed in [15], can be very useful in reducing bias errors to a large extent. Even using a bias control solution, some residual bias errors could still be present. Once again, if the signal has a suboctave bandwidth, second-order nonlinearities fall outside the signal band. Simulation result shown in Fig. 7 includes a bias error of 5° .

VI. CONCLUSION

The TS-ADC has tremendous potential for digitizing signals with very high bandwidths. The system, however, suffers

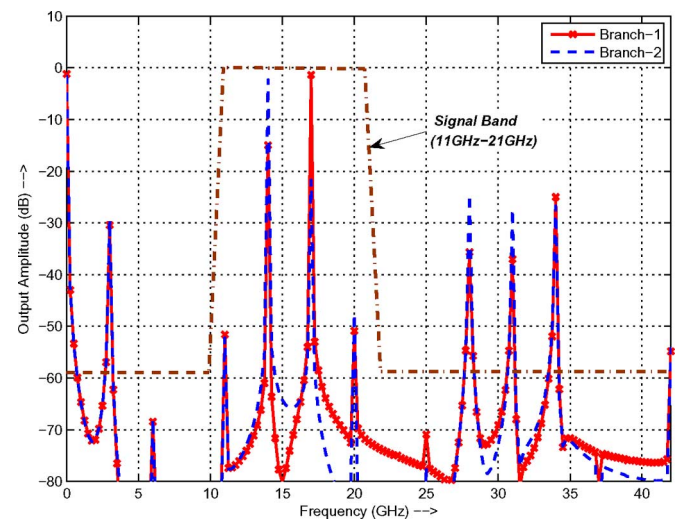


Fig. 7. Two-tone spectrum for a modulation depth of $m = 0.2$ showing third-order intermods falling within and second-order harmonic and intermod tones falling outside the 11–21-GHz passband. The horizontal axis is the effective input frequency, i.e., it does not reflect the 10 \times reduction in the center frequency and the bandwidth.

from the frequency-selective nature of the time-stretch process, which is an effect that limits its dynamic range in wideband applications. It was shown in this paper that 2-D spatio-temporal digital processing can be used to overcome this limitation. Due to its adaptive nature, the solution is robust with respect to non-idealities in the transfer characteristics of the optical system.

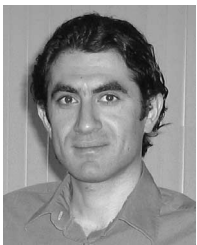
ACKNOWLEDGMENT

The authors would like to thank J. Chou for helpful discussions.

REFERENCES

- [1] R. H. Walden, "Analog-to-digital converter survey and analysis," *IEEE J. Sel. Areas Commun.*, vol. 17, no. 4, pp. 539–550, Apr. 1999.
- [2] W. C. Black and D. A. Hodges, "Time interleaved converter arrays," *IEEE J. Solid-State Circuits*, vol. SSC-15, no. 6, pp. 1022–1029, Dec. 1980.
- [3] A. Montijo and K. Rush, "Accuracy in interleaved ADC systems," *Hewlett-Packard J.*, vol. 44, no. 5, pp. 38–46, Oct. 1993.

- [4] P. W. Juodawlkis, J. C. Twichell, G. E. Betts, J. J. Hargreaves, R. D. Younger, J. L. Wasserman, F. J. O'Donnell, K. G. Ray, and R. C. Williamson, "Optically sampled analog-to-digital converters," *IEEE Trans. Microw. Theory Tech.*, vol. 49, no. 10, pp. 1840–1853, Oct. 2001.
- [5] J. C. Twichell and R. Helkey, "Phase-encoded optical sampling for analog-to-digital converters," *IEEE Photon. Technol. Lett.*, vol. 12, no. 9, pp. 1237–1239, Sep. 2000.
- [6] W. J. Caputi, "Stretch: A time-transformation technique," *IEEE Trans. Aerosp. Electron. Syst.*, vol. AES-7, no. 2, pp. 269–278, Mar. 1971.
- [7] B. Jalali and F. Coppinger, "Data conversion using time manipulation," U.S. Patent 6 288 659, Sep. 11, 2001.
- [8] F. Coppinger, A. S. Bhushan, and B. Jalali, "Photonic time stretch and its application to analog-to-digital conversion," *IEEE Trans. Microw. Theory Tech.*, vol. 47, no. 7, pp. 1309–1314, Jul. 1999.
- [9] A. S. Bhushan, P. V. Kelkar, B. Jalali, O. Boyraz, and M. Islam, "130 GSa/s photonic analog-to-digital converter with time stretch pre-processor," *IEEE Photon. Technol. Lett.*, vol. 14, no. 5, pp. 684–686, May 2002.
- [10] Y. Han and B. Jalali, "Photonic time-stretched analog-to-digital converter: Fundamental concepts and practical considerations," *J. Lightw. Technol.*, vol. 21, no. 12, pp. 3085–3103, Dec. 2003.
- [11] O. Boyraz, J. Kim, M. N. Islam, F. Coppinger, and B. Jalali, "Broadband, high-brightness 10-Gb/s supercontinuum source for A/D conversion," in *Proc. Lasers Electro-Opt. Conf.*, 2000, pp. 489–490.
- [12] Y. Han, O. Boyraz, and B. Jalali, "Ultrawide-band photonic time-stretch A/D converter employing phase diversity," *IEEE Trans. Microw. Theory Tech.*, vol. 53, no. 4, pp. 1404–1408, Apr. 2005.
- [13] A. H. Sayed, *Fundamentals of Adaptive Filtering*. New York: Wiley, 2003.
- [14] Analog Devices Engineering Staff, *Data Conversion Handbook*, New York: Elsevier, 2005.
- [15] J. Basak, R. Sadhwani, and B. Jalali, "WDM pilot tone technique for analog optical links," *Electron. Lett.*, vol. 39, no. 14, pp. 1083–1084, Jul. 2003.



Alireza Tarighat (S'00–M'05) received the B.Sc. degree in electrical engineering from Sharif University of Technology, Tehran, Iran, in 1998, and the M.Sc. and Ph.D. degrees in electrical engineering from University of California, Los Angeles (UCLA), in 2001 and 2005, respectively.

During the summer of 2000, he was with Broadcom, El Segundo, CA, where he worked on IEEE 802.11 transceivers. From 2001 to 2002, he was with Innovics Wireless, Los Angeles, CA, working on system and application-specified integrated circuit

development of advanced antenna diversity and rake processing for 3G wideband-code-division-multiple-access mobile terminals. Since 2005, he has been at WiLinX, Los Angeles, CA, working on system and silicon development of ultrawideband wireless networks. His research interests are in communication theory and signal processing, including multiple-input multiple-output (MIMO) orthogonal frequency-division multiplexing systems, multiuser MIMO wireless networks, algorithms for impairments compensation, and experimental and practical communication systems.

Dr. Tarighat was the recipient of the Gold Medal of the National Physics Olympiad, Iran, in 1993, and the Honorable Mention Diploma of the 25th International Physics Olympiad, Beijing, China, in 1994. He received the 2006 Outstanding Ph.D. Dissertation Award in electrical engineering from UCLA.



Shalabh Gupta (S'03) received the B.Tech degree in electrical engineering from the Indian Institute of Technology, Kanpur, India, in 2001 and the M.S. degree in electrical engineering from the University of California, Los Angeles (UCLA), in 2004. He is currently working toward the Ph.D. degree in electrical engineering at UCLA, where his research focus is in the field of microwave photonics.

In August 2003, he was with Chrontel, Inc., San Jose, CA, where he primarily designed the analog integrated circuits for high-speed serial links. Before

joining the Optoelectronics Circuits and Systems Laboratory at UCLA to pursue the Ph.D. degree, he also worked at Skyworks Solutions, Inc., Irvine, CA, as a Senior Electrical Engineer for radio frequency integrated circuits. At Skyworks, he contributed to the design and development of global systems for mobile communications/enhanced data rates for GSM evolution transceiver chipsets. His research interests include analog/RF integrated circuits, beam-forming antennas, and microwave photonics.



Ali H. Sayed (F'01) received the Ph.D. degree in electrical engineering from Stanford University, Stanford, CA, in 1992.

He is a Professor and Chairman of electrical engineering at the University of California, Los Angeles (UCLA). He is also the Principal Investigator of the UCLA Adaptive Systems Laboratory. He has over 250 journal and conference publications, is the author of the textbook *Fundamentals of Adaptive Filtering* (New York: Wiley, 2003), and is the coauthor of the research monograph *Indefinite Quadratic Estimation and Control* (Philadelphia, PA: SIAM, 1999) and of the graduate-level textbook *Linear Estimation* (Englewood Cliffs, NJ: Prentice-Hall, 2000). He is also the coeditor of the volume *Fast Reliable Algorithms for Matrices With Structure* (Philadelphia, PA: SIAM, 1999). He has contributed several articles to engineering and mathematical encyclopedias and handbooks and has served on the program committees of several international meetings. His research interests span several areas, including adaptive and statistical signal processing, filtering and estimation theories, signal processing for communications, interplays between signal processing and control methodologies, system theory, and fast algorithms for large-scale problems.

Dr. Sayed was the recipient of the 1996 IEEE Donald G. Fink Award, the 2002 Best Paper Award from the IEEE Signal Processing Society, the 2003 Kuwait Prize in Basic Science, the 2005 Frederick E. Terman Award, the 2005 Young Author Best Paper Award from the IEEE Signal Processing Society, and two Best Student Paper Awards at international meetings. He is also a member of the technical committees on Signal Processing Theory and Methods and on Signal Processing for Communications, both of the IEEE Signal Processing Society. He is a member of the editorial board of the IEEE SIGNAL PROCESSING MAGAZINE. He served as Editor-in-Chief of the IEEE TRANSACTIONS ON SIGNAL PROCESSING from 2003 to 2005 and is now serving as Editor-in-Chief of the European Association for Signal Processing *Journal on Applied Signal Processing*. He is serving as General Chairman of the International Conference on Acoustics, Speech, and Signal Processing, 2008.



Bahram Jalali (F'04) received the M.S. and Ph.D. degrees in applied physics from Columbia University, New York, NY, in 1986 and 1989, respectively.

He is a Professor of electrical engineering and the Director of the Optoelectronic Circuits and System Laboratory, University of California, Los Angeles (UCLA). From 1988 to 1992, he was a member of the Technical Staff at the Physics Research Division of AT&T Bell Laboratories, Murray Hill, NJ, where he conducted research on ultrafast electronics and optoelectronics. His current

research interests are in silicon photonics and ultrafast photonic signal processing. He has published over 200 scientific papers and is the holder of six U.S. patents. In 2005, he was chosen by Scientific American Magazine as one of the 50 Leaders Shaping the Future of Technology. While on leave from UCLA from 1999 to 2001, he founded Cognet Microsystems, which is a Los Angeles-based fiber optic component company. He served as the Company's CEO, President, and Chairman from the company's inception through its acquisition by Intel Corporation in April 2001. From 2001 to 2004, he served as a Consultant to Intel Corporation. He also serves on the Board of Trustees of the California Science Center.

Dr. Jalali is a Fellow of Optical Society of America and the Chair of the Los Angeles Chapter of the IEEE Lasers and Electro Optics Society. He is a member of the California Nano Systems Institute. He was the recipient of the BridgeGate 20 Award for his contribution to the Southern California economy.